Correlation of the exchange interaction in $Ni_{81}Fe_{19}/Cr_2O_3$ bilayers with the antiferromagnetic spin configuration

Joonghoe Dho* and M. G. Blamire†
Department of Materials Science and Metallurgy, University of Cambridge, Pembroke Street, Cambridge CB2 3QZ, United Kingdom

E. O. Chi
Department of Chemistry, University of Houston, 136 Fleming Building, Houston, Texas 77204-5003, USA
(Received 14 July 2005; revised manuscript received 20 October 2005; published 15 December 2005)

The exchange interaction and the resulting exchange bias between ferromagnet and antiferromagnet layers are fundamental to the operation of magnetic data storage devices. Despite considerable work, and the development of many theoretical models, quantitative agreement between theory and experiment is still poor. Here we report a systematic comparison between experiments on $Ni_{81}Fe_{19}$/epitaxial Cr_2O_3 bilayers and a phenomenological model of the effect which can fit experimental data and enables key ingredients of previous rigorous models to be applied to experimental data. Our results show unambiguously that the uniaxial anisotropy which leads to enhanced coercivity in most exchange-coupled systems and the exchange bias have fundamentally independent origins and that only a very restricted subset of possible crystal orientations can result in a large exchange bias. These factors are masked in experiments on polycrystalline systems and on rough interfaces in single-crystalline systems.

DOI: 10.1103/PhysRevB.72.224421 PACS number(s): 75.30.Et, 75.50.Ss, 75.70.Cn

I. INTRODUCTION

The phenomenon of exchange bias is fundamental to the operation of various magnetic devices; notably spin valves for data read-out from magnetic hard discs, and spin tunnel junctions for magnetic random access memory. Exchange bias is the shift of the magnetic reversal loop away from zero applied field (by an amount defined as the exchange bias field H_{ex}) so that the biased layer does not reverse on the operating field range of the device. It is induced in a ferromagnet (FM) by an exchange interaction with an adjacent antiferromagnet (AF). Despite the immense technological importance of the effect and considerable research spanning two decades, the predictive power of models for the exchange interaction is still at best rudimentary.[1,2] There is considerable technological pressure to increase the strength of exchange bias and to increase the temperature range over which it operates. It has been demonstrated as a technique to stabilize FM nanoparticles below the superparamagnetic limit.[3]

The earliest theory of exchange bias[4] compared the ionic exchange interaction energy across the interface with the Zeeman energy of the FM in applied field. In its simplest form, this model is clearly inappropriate since it predicts a zero value for H_{ex} for spin-compensated AF interfaces which often show a significant bias and, for uncompensated interfaces, grossly overestimates the magnitude of the effect compared to experimental results. The models of Malozemoff[5] and Mauri[6] were introduced to overcome these discrepancies, the former introduces disorder associated with surface roughness and the domain state of the AF to predict a finite H_{ex} for compensated interfaces, while the latter introduces domain wall structures in the AF to reduce the total H_{ex}.

Experimentally it has been observed that the exchange interaction often substantially increases the coercive field (H_C) of the FM. The models of Koon[7] and Schulthess and Butler[8,9] are based on the exchange coupling to a compensated AF surface so as to induce a surface relaxation of the AF spins akin to the spin-flop interaction of an AF with a large applied field. This spin-flop coupling gives rise to a uniaxial anisotropy perpendicular to the spin direction of the AF and results in such an enhanced coercivity.[16,17] This anisotropy has been experimentally observed.[10,11] An enhanced coercivity associated with short-range AF order above T_N has recently been observed in Fe/FeF_2.[12] Interestingly, a very recent paper of Borisov *et al.* has demonstrated an electrically switchable exchange bias in the magnetoelectric Cr_2O_3.[13–15]

However none of these models, or their successors, provide any general predictive capability. There are three fundamental reasons for this. First, most experimental results are derived from polycrystalline AFs, which necessarily average over the different anisotropy directions in the AF. Second, in experiments performed on epitaxial AFs[10,11,16–21] variable exchange bias is seen in compensated interfaces and is surprisingly absent in some experiments on uncompensated interfaces.[19] Finally, the very short-range nature of the effect means that surface roughness, even at subunit cell levels, is sufficient to alter the magnitude of the effect drastically.[21] To these must be added the very considerable experimental problem that, except in very special circumstances, there are very few direct probes of the micromagnetic structure of the AF (Refs. 18, 22, and 23) and so the state of the AF must be inferred via the incompletely understood exchange interaction itself.

Systematic study of exchange bias therefore requires an much improved experimental system and a better understanding of the properties of the AF and the FM. In this paper we report results from a system which we believe satisfied these requirements, in which epitaxial Cr_2O_3 is the AF and

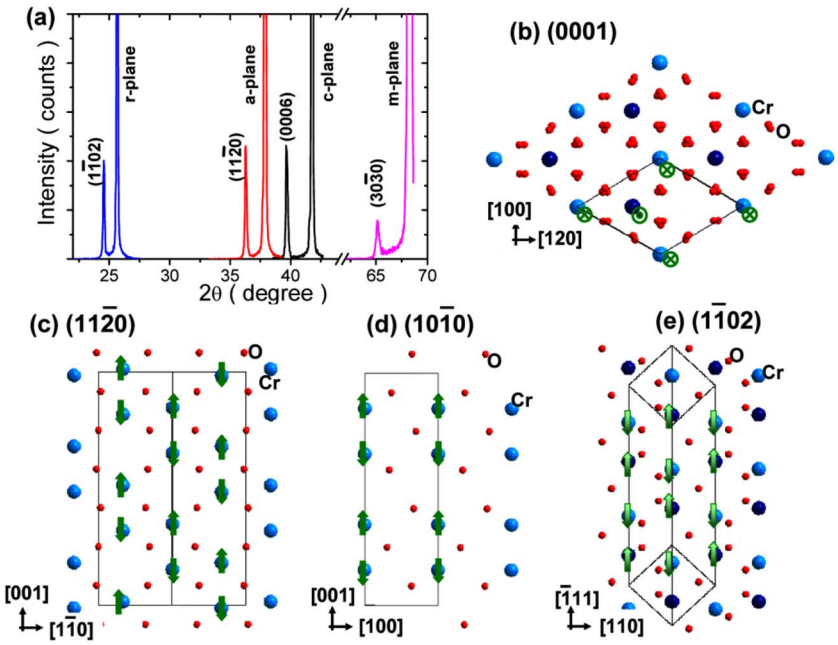

FIG. 1. (Color online) (a) XRD patterns for the (0001), $(11\bar{2}0)$, $(10\bar{1}0)$, and $(1\bar{1}02)$ Cr_2O_3 on *c*-plane, *a*-plane, *m*-plane, and *r*-plane Al_2O_3 substrates. The in-plane atomic and spin structure for the (b) (0001), (c) $(11\bar{2}0)$, (d) $(10\bar{1}0)$, and (e) $(1\bar{1}02)$ Cr_2O_3. Large light blue (gray) and small red (gray) balls display the Cr and the O atoms, respectively. Large light blue (gray) Cr atoms are exactly in the plane defined, while the large dark blue (black) Cr atoms are located slightly below the plane. The green (gray) arrow and crossed circle display the Cr spins. The gradient green (gray) arrows in (e) imply that the Cr spins are tilting to the plane.

permalloy ($Ni_{81}Fe_{19}$) is the FM. We show that, because all the anisotropy in the experimental results must derive from the AF, we can use a simple phenomenological model to fit the FM reversal loops under a wide variety of annealing and measurement configurations.

II. EXPERIMENT

A. Sample preparation

Chromium oxide Cr_2O_3 is a hexagonal AF with a Néel temperature $T_N \sim 307$ K and a robust uniaxial anisotropy.[24–26] Cr_2O_3 grows epitaxially on α-Al_2O_3 (sapphire) with a lattice mismatch of ~4.2% and is thus an excellent system with which to study the effect of different interfacial AF spin configurations on exchange bias and coercivity. Permalloy has minimal magnetocrystalline anisotropy and a high Curie temperature.

Epitaxial and polycrystalline Cr_2O_3 films were grown on *c*-plane (0001), *a*-plane $(11\bar{2}0)$, *m*-plane $(10\bar{1}0)$, *r*-plane $(1\bar{1}02)$ α-Al_2O_3, and Si substrates by pulsed laser deposition (PLD) with a substrate temperature of 973 K and oxygen pressure of 0.2–20 mTorr. The 60 nm thick Cr_2O_3 films were transferred into an ultrahigh vacuum dc sputtering chamber and a 5 nm polycrystalline permalloy film was deposited on them at room temperature. The surface roughness of Cr_2O_3 layers was measured by atomic force microscopy.

B. Structural characterisation

Figure 1(a) shows x-ray diffraction (XRD) data for the epitaxial Cr_2O_3 layers. All four epitaxial growth directions yielded untwinned films with excellent crystallinity with a full-width-at-half-maximum of ~0.09° and ~0.8° in the rocking curve and in the ϕ scan, respectively. The lattice parameters of all the epitaxial Cr_2O_3 films agreed with those of bulk Cr_2O_3 material (a=4.961 Å, c=13.595 Å) to within ~0.2%, indicating that the lattice mismatch strain was fully relaxed. Therefore, it is reasonable to assume that the epitaxial Cr_2O_3 samples have the same AF spin order as bulk crystals.[24–26] Figures 1(b)–1(e) show the atomic structure and spin configuration within the plane for different orientations. Here, we reconstruct the spin structure for each orientation in hexagonal representation from the well-known AF spin structure in rhombohedral representation.[24,25] The $(11\bar{2}0)$ and $(10\bar{1}0)$ orientations are fully compensated surfaces with in-plane spin, while the (0001) and $(1\bar{1}02)$ orientations are uncompensated but can easily become effectively compensated through surface roughness exposing neighboring planes which have antiparallel spins [dark blue in Figs. 1(b) and 1(e)]. The AF spins in $(11\bar{2}0)$ and $(10\bar{1}0)$ Cr_2O_3 are parallel to the interface, while those in the (0001) Cr_2O_3 are perpendicular to the interface and those in the $(1\bar{1}02)$ Cr_2O_3 are tilted with an angle (~32.3°) to the interface.

III. RESULTS AND EXCHANGE INTERACTION MODEL

A. Results on exchange bias and coercivity

Magnetic measurements were performed using a variable-temperature vibrating sample magnetometer (VSM). The samples were cooled down from 350 K (above T_N) to 77 K in an annealing magnetic field (H_A) of 1 kOe, and magnetization vs magnetic field loops were collected upon warming.

Previously, only a weak exchange interaction has been observed on an uncompensated surface, in contradiction to the simplest model for such systems.[16] We were able to control the surface roughness of (0001) Cr_2O_3 layers by altering the oxygen pressure during growth. As seen in Fig. 2, exchange bias and coercivity for the (0001) Cr_2O_3 increase rapidly as the surface roughness decreases, demonstrating that the exchange interaction is rapidly averaged out by surface roughness. In order to measure the intrinsic properties of

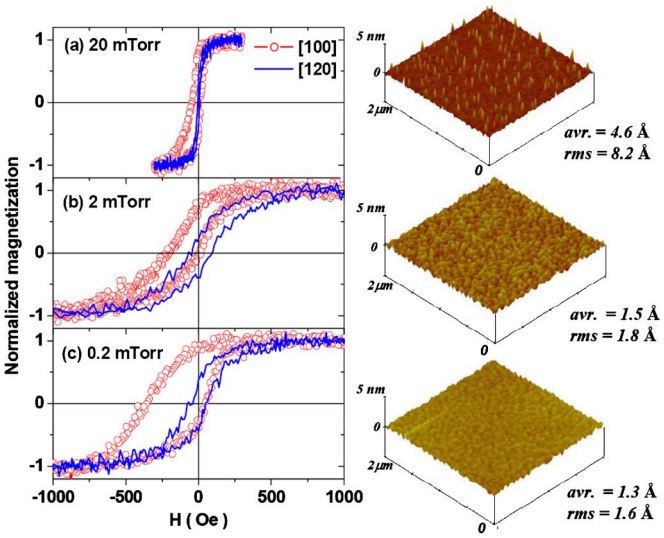

FIG. 2. (Color online) Left panel, magnetic hysteresis loops for $Ni_{81}Fe_{19}$ layers on the (0001) Cr_2O_3 which are grown at different oxygen pressures. The measurement temperature was 77 K. Right panel, AFM images of the (0001) Cr_2O_3 layer for different oxygen pressures. The avr. and rms indicate average roughness and root mean square roughness, respectively.

uncompensated surfaces it is therefore essential to minimize the roughness. At a growth pressure of 0.02 mTorr, the (0001) Cr_2O_3 showed a very small average roughness of ~1.3 Å and displayed large values of exchange bias and coercivity.

Figure 3 shows temperature-dependent magnetic hysteresis loops for the different growth orientations with optimized surfaces; each panel shows data collected for two orthogonal in-plane directions, in each case parallel and perpendicular to the field-cooling direction. At 77 K the exchange bias and coercivity depend strongly on the Cr_2O_3 orientations and the measurement direction. The (0001) orientation displayed large values of $H_{ex} \sim 165$ Oe and $H_C \sim 200$ Oe [Fig. 3(a)]; in the $(11\bar{2}0)$ and $(10\bar{1}0)$ orientations, which have rather similar surface spin configurations, a large H_C of 440–540 Oe was observed but the H_{ex} was small at around 15–30 Oe [Figs. 3(b) and 3(c)]. Finally the $(1\bar{1}02)$ orientation displayed a large H_{ex} of ~600 Oe at 77 K but a small H_C of ~60 Oe [Fig. 3(d)]. The polycrystalline Cr_2O_3 layer displayed intermediate values of exchange bias and coercivity in comparison with the epitaxial ones [Fig. 3(e)]. By 350 K, above T_N, the exchange bias had vanished as expected, but the coercivity remained strongly dependent on the orientation. The pronounced hard and easy axes are indicative of a strong residual exchange interaction above T_N.

The $(11\bar{2}0)$ and $(10\bar{1}0)$ orientations have only an *in-plane* spin component and do not show exchange bias irrespective of the direction of annealing field. In Fig. 4, magnetic hsyteresis loops do not show much difference for two orthogonal in-plane annealing fields, except slight changes in squareness of loops and coercivity. On the other hand, the (0001) and $(1\bar{1}02)$ orientations both have an out-of-plane spin component, but their exchange coupling to Py is clearly different.

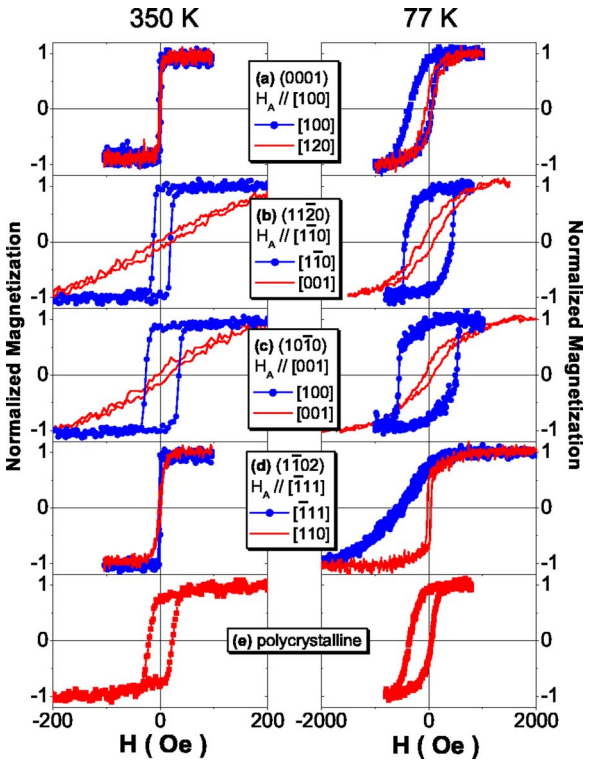

FIG. 3. (Color online) Magnetic hysteresis loops for $Ni_{81}Fe_{19}$ layers (a) on (0001) Cr_2O_3, (b) on $(11\bar{2}0)$ Cr_2O_3, (c) on $(10\bar{1}0)$ Cr_2O_3, (d) on $(1\bar{1}02)$ Cr_2O_3, and (e) on polycrystalline Cr_2O_3 at 350 K and 77 K. H_A is the magnetic field direction during cooling. For these experiments, the sample (a) was grown at 20 mTorr while the others were done at 20 mTorr. The average roughness was ~1.3 Å for the sample (a), ~4.5 Å for the samples (b) and (c), ~7.5 Å for the sample (d), and ~25 Å for the sample (e), respectively.

In the (0001) orientation, exchange bias can be induced in all in-plane directions by appropriate magnetic field cooling through T_N; in this case the AF spins align perpendicular to the interface, and so there is negligible anisotropy within the plane. The behavior of the anisotropic $(1\bar{1}02)$ orientation was studied as a function of field annealing direction. Figure 5(a) shows the evolution of the magnetic hysteresis loops as the magnetic field cooling direction is varied between the $[\bar{1}11]$ and [110] directions. Figure 5(b) shows measurements parallel and perpendicular to the magnetic field cooling along the $[\bar{1}11]$ and [110] directions; a large exchange bias appeared only in a specific direction parallel or anti-parallel to the $[\bar{1}11]$ direction. More remarkably, bias also appeared along the $[\bar{1}11]$ direction even when the magnetic field cooling was performed approximately perpendicular to it as shown in Fig. 5(c). This is very unusual because conventional exchange biased systems typically show an exchange bias parallel to the field cooling direction.

Figure 6 shows the temperature dependences of the exchange bias and coercivity for the specific directions on the different Cr_2O_3 orientations. As the temperature increases, the coercivity and exchange bias substantially drop around $T \sim 305$ K, which agrees with the T_N of bulk Cr_2O_3.[19–21] For

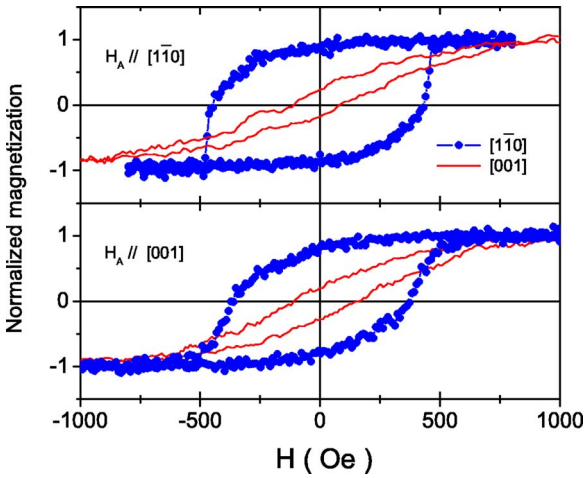

FIG. 4. (Color online) Magnetic hysteresis loops for $Ni_{81}Fe_{19}$ layers on $(11\bar{2}0)$ Cr_2O_3 (a) with $H_A//[1\bar{1}0]$ and (b) with $H_A//[001]$. For these measurements, the sample was cooled down to 77 K with the H_A parallel to a specific direction.

comparison, the temperature-dependent dc magnetic susceptibility of our target material Cr_2O_3 was displayed in Fig. 6(f). The coercivity in the $(1\bar{1}02)$ orientation has a clear peak around T_N and in the (0001) orientation an excess coercivity compared with the exchange bias appears in the same temperature range. In contrast, in the other orientations the coercivity monotonically decreases to T_N, but remains at a high residual level above it.

The magnitudes of the exchange bias and coercivity with different Cr_2O_3 orientations at 77 K are summarized in Table I. The maximum exchange bias energy is about 0.27 erg/cm^2 at ~200 K for the $(1\bar{1}02)$ Cr_2O_3; this value is similar to that for polycrystalline CoO.[2] On the other hand, the maximum coercivity was about 540 Oe for the $(10\bar{1}0)$ Cr_2O_3.

B. Exchange interaction model

The most significant behavior is that observed in the $(1\bar{1}02)$ orientation, in which the exchange bias only appears along a specific in-plane direction, associated with the tilting of the AF spins along the *c*-axis direction [Fig. 1(e)] and perpendicular to the easy axis identified with spin-flop coupling. The angle-dependent data shown in Fig. 5(a), which appear to be a combination of two loops associated with orthogonal principal axes, strongly suggest that these anisotropy axes act independently.

To illustrate the effects at work we have developed a phenomenological model to describe the behavior. We start by considering the total energy of the FM within the exchange-coupled system,

$$E_{\mathrm{FM}} = -t\mathbf{M}\cdot\mathbf{H} - j(\mathbf{M}\cdot\mathbf{m_d} + |\mathbf{M}\cdot\mathbf{m_a}|). \quad (1)$$

Here the first term is the usual Zeeman energy with **H** and **M** the magnetic field and saturation magnetization, respectively, *t* is the FM thickness, *j* is the strength of the exchange interaction between the AF and FM and $\mathbf{m_d}$ and $\mathbf{m_a}$, respectively, represent the net spin in the AF along axes which correspond

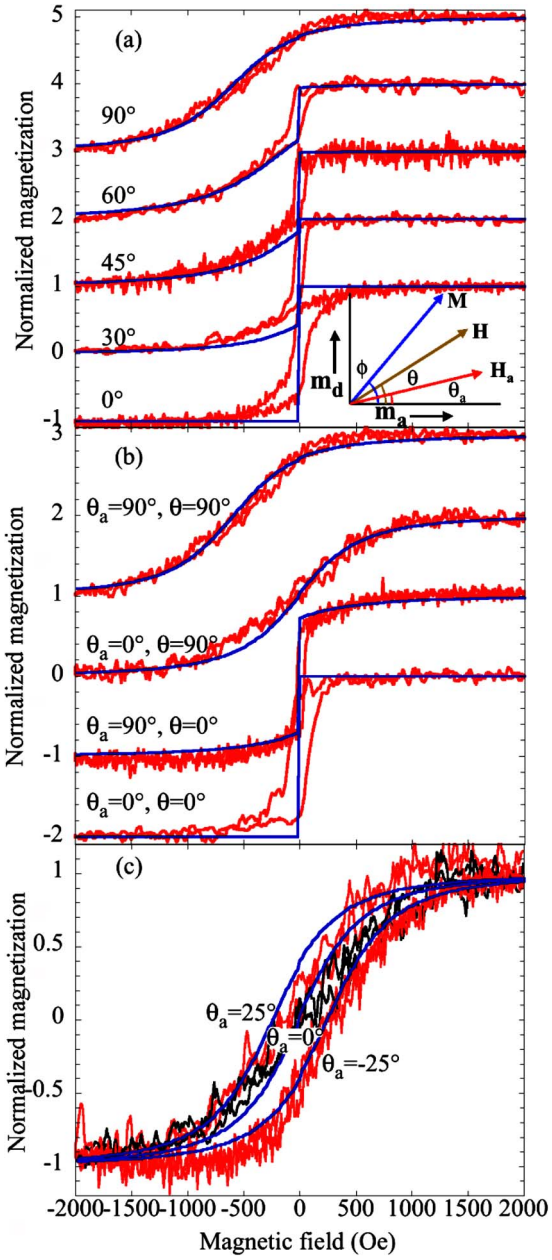

FIG. 5. (Color online) Magnetic hysteresis loops measured (red noisy lines) for $Ni_{81}Fe_{19}$ layers on the $(1\bar{1}02)$ Cr_2O_3 under various conditions, (a) with a magnetic field cooling direction parallel to the measurement direction and aligned along various Cr_2O_3 in-plane directions between $[\bar{1}11]$ and [110] (angles measured with respect to [110]); (b) with a magnetic field cooling along the $[\bar{1}11]$ and the [110] directions, the measurements were performed parallel and perpendicular to the cooling direction in each case; (c) with the magnetic cooling direction close to [110] and measured along $[\bar{1}11]$. In each case the smooth (blue) lines represent fits using the model described in the text. The curves in (a) and (b) are successively shifted by 1 unit on the *y* axis.

to the orthogonal directions of the unidirectional and spin-flop uniaxial anisotropies, respectively [see inset to Fig. 5(a)]. We have used the $j|\mathbf{M}\cdot\mathbf{m_a}|$ notation instead of the

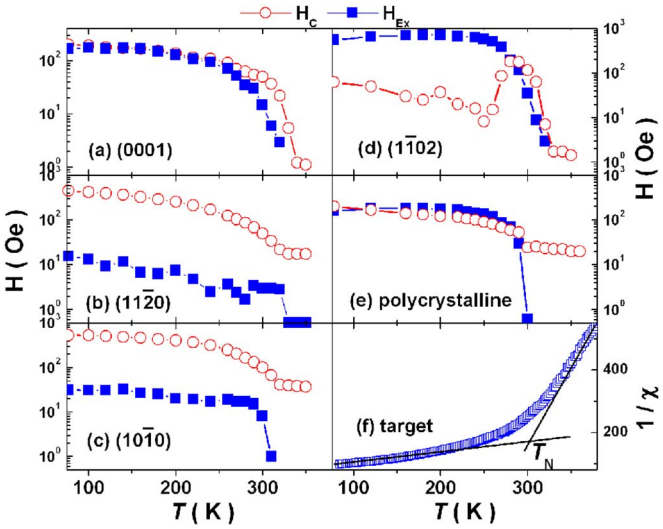

FIG. 6. (Color online) The temperature dependence of the exchange bias (H_{ex}) and the coercivity (H_C) of $Ni_{81}Fe_{19}$ on (a) on (0001) Cr_2O_3, (b) on (11$\bar{2}$0) Cr_2O_3, (c) on (10$\bar{1}$0) Cr_2O_3, (d) on (1$\bar{1}$02) Cr_2O_3, and (e) on polycrystalline Cr_2O_3. The temperature dependence of the inverse dc magnetic susceptibility ($1/\chi$) for our target material Cr_2O_3 was displayed in (f). The AF transition temperature (T_N) was roughly determined by linear fits of $1/\chi$ for high and low temperature regions.

more usual cosine squared expression for uniaxial anisotropy for reasons that will be discussed later.

Similarly we can define the energy of the exchange-coupled AF,

$$E_{AF} = -j(\mathbf{M}\cdot\mathbf{m_d} + |\mathbf{M}\cdot\mathbf{m_a}|) + km_d^2, \tag{2}$$

where the first term again represents the interfacial exchange coupling. The second term reflects the fact that in a real system all AF surfaces are effectively compensated, either intrinsically, by roughness or by the domain structure of the AF, and so a magnetic disorder must be induced in the AF, which raises the energy of the system; the quadratic dependence is based on a simple elastic model for such energy. This magnetic disorder disrupts the long-range order within the AF and is most naturally associated with the domain state model of Nowak *et al.*[27]

To apply this model we assume that a magnetic field cooling process is performed with the FM saturated along the direction (θ_a) of the annealing field relative to the uniaxial anisotropy axis so that

$$E_{AF} = -jM(m_d \sin\theta_a + m_a|\cos\theta_a|) + km_d^2 \tag{3}$$

and minimize E_{AF} with respect to m_d so that

$$m_d = \frac{jM\sin\theta_a}{2k}. \tag{4}$$

We make the usual assumption that well below T_N the AF is unaffected by subsequent changes in the FM magnetization; therefore this value of m_d can be substituted into (1) to give

$$\frac{E_{FM}}{M} = -tH\cos(\phi-\theta) - \frac{j^2M}{2k}\sin\theta_a\sin\phi - jm_a|\cos\phi|, \tag{5}$$

where θ is the angle of the measurement field to the uniaxial anisotropy axis and ϕ is the angle of the magnetization to the uniaxial anisotropy axis.

The model therefore has two adjustable parameters A ($=jm_a$) and D ($=j^2M/2k$). As in any potentially hysteretic system we have the choice of local or global minimization; the coercivity observed in the (1$\bar{1}$02) orientation is relatively weak, and so we globally minimize the energy (5) with respect to ϕ and plot magnetization loops by taking the component $M\cos(\phi-\theta)$ as the measured magnetization. Using a single value throughout for A and D we have calculated fits for the data shown as continuous lines in Fig. 5. The loops were quite asymmetric similar to Camarero's report based on coherent rotation model.[28] Parameters D and A determine the degree of bias and spin-flop coupling, respectively, through the exchange stiffness k of the AF and the net spin-flop moment m_a. In these fits we used values of A and D of 400 Oe and 600 Oe, respectively, assuming the 5 nm film thickness.

Apart from the artificial elimination of the small coercivity, the agreement with the experimental data is striking. In particular, the fact that we can model all the data in Fig. 5 assuming a constant value for the spin-flop and bias constants A and D demonstrates the degree to which these two phenomena are decoupled in this system. This model can be shown to agree with the rest of the data presented if we make the reasonable assumption that D is much smaller for the compensated interfaces and that A is zero for the isotropic (0001) surface.

TABLE I. Exchange bias and coercivity with the orientation of Cr_2O_3 layers at 77 K.

Cr_2O_3	H_C(erg/cm)	H_{ex}(erg/cm)
(0001)	0.078	0.066
(11$\bar{2}$0)	0.176	0.006
(10$\bar{1}$0)	0.207	0.012
(1$\bar{1}$02)	0.023	0.215
Polycrystalline	0.078	0.062

IV. DISCUSSION

The results in this paper, although superficially at odds with some other experiments on epitaxial antiferromagnets, fit very well with a simple model that includes spin-flop-induced anisotropy and exchange bias as independent phenomena. In this section we discuss these results and the underlying requirements for significant and applicable exchange bias.

A. Enhanced coercivity

It is a general feature of polycrystalline exchange-bias systems that there is a substantial additional coercivity com-

pared with single FM layers. Stiles and McMichael[29] distinguish between an additional coercivity, which is largest close to the blocking temperature (associated with spin reversal in the AF), and a low temperature coercivity, which is associated with inhomogeneous coupling between the FM and AF. There is good evidence that much of the low temperature coercivity is associated with a uniaxial anisotropy induced by spin-flop coupling with a compensated AF surface.

We start by distinguishing between exchange-induced uniaxial anisotropy and enhanced coercivity. For all of our samples except those in which there is no in-plane crystal anisotropy [polycrystalline and (0001) films], there is a very strong uniaxial anisotropy induced in the Py (Fig. 3). In each case this anisotropy axis is normal to the AF spin direction and so it can be ascribed directly to Koon's spin-flop coupling.[7] Two of the surfaces that show this anisotropy are fully compensated, but $(1\bar{1}02)$ is uncompensated, but with an offset antiparallel spin plane very close to the surface [see Fig. 1(e)]. It seems that both (antiparallel) planes couple to the FM and so undergo a spin-flop relaxation.

For systems that reverse coherently, a uniaxial anisotropy directly translates into a maximal coercivity along the easy axis. For the compensated $(11\bar{2}0)$ and $(10\bar{1}0)$ surfaces in Figs. 3(b) and 3(c) we can accurately fit the hard axis data using (5) by setting the bias constant D to zero to reflect the absence of bias in these surfaces and adjusting the spin-flop constant A. Using the fitted values of A and assuming coherent reversal by taking a local rather than global energy minimum in (5) we can calculate easy axis coercivities of 500 Oe and 600 Oe, respectively, compared with experimental values of 450 Oe and 520 Oe. This close agreement suggests the domain wall nucleation or movement is strongly inhibited on such compensated interfaces. In contrast, the induced low temperature coercivity along the easy axis is much lower for the $(1\bar{1}02)$ surface, which shows a large exchange bias. Partly this reflects a reduced spin-flop coupling arising from the destabilizing effect of the orthogonal unidirectional anisotropy, but it is clear that in this case FM domain wall reversal must dominate.

Interestingly, the magnetic hysteresis loops for the $(11\bar{2}0)$ and $(10\bar{1}0)$ orientations showed strong anisotropy and enhanced coercivity even above T_N (left-hand panels of Fig. 3 and Fig 5); similar behavior has been observed previously in the epitaxial system Fe/FeF_2.[12] For Cr_2O_3, this is presumably due to a short range AF coupling between the two most-closely coupled Cr ions: in these orientations, these ions lie in the plane of the surface, while in the $(1\bar{1}02)$ orientation the spins are in neighboring planes [see Figs. 1(c)–1(e)]. This difference is consistent with the large anisotropy and coercivity in the first two orientations and the weaker behavior in the latter. Further support for this comes from the rotation of the easy axis in the $(1\bar{1}02)$ orientation below and above T_N: in the $(1\bar{1}02)$ orientation, the long range AF order below T_N is parallel to the c-axis direction. Above T_N, however, the average short range AF coupling perpendicular to the c-axis seems to be slightly stronger than that parallel to the c axis because the average Cr-Cr distance is slightly longer along the c axis.

B. Exchange bias

Our model assumes that significant exchange bias requires uncompensated interfaces. Although substantial bias from compensated single-crystal CoO interfaces has been reported,[18,21,30] there is good evidence that this is a consequence either of degraded epitaxy, which leads to local uncompensation,[21] or because the 90° spin-flop coupling of Koon[7] can be stabilized in some systems so as to lie perpendicular to the net spin direction.[18] It is consistent with this that in both of these cases, the coercivity is much larger than the net bias showing that the uniaxial anisotropy associated with spin-flop reversal is active over much of the interface.

In contrast to these earlier experiments, Cr_2O_3 has a uniaxial anisotropy and our films were grown so that the uncompensated plane $(1\bar{1}02)$ was untwinned. Thus we know that for the $(1\bar{1}02)$ plane precisely which direction any bias due to uncompensation should arise and that the only effect of the AF micromagnetic structure is to modify the net spin pointing along the $[\bar{1}11]$ direction. Our results show clearly that the bias is aligned with this direction even when the cooling field is at a large angle to it and so the bias in this experimental system must arise from a net uncompensation of the surface, which can easily be degraded by surface roughness. This is also consistent with our previous report on the epitaxial AF system $Ni_{81}Fe_{19}/\alpha\text{-}Fe_2O_3$.[20]

C. The independence of coercivity and exchange bias

The results of these measurements may be summarized by noting that all the Cr_2O_3 planes which have an anisotropic in-plane spin configuration show a pronounced anisotropy in the exchange interaction with the FM easy axis lying perpendicular to the AF spin axis. Significant exchange bias only occurs on certain crystal planes of Cr_2O_3 that have uncompensated surfaces. For the (0001) orientation that has minimal in-plane anisotropy an exchange bias can be induced in parallel to any magnetic field cooling direction.

This allows us to link our phenomenological model to existing analytical models for the exchange interaction. We can clearly identify A with the Koon spin-flop interaction, which has a very definite direction with respect to that of the spin direction of the AF.[7] The form of the uniaxial anisotropy used in the model does not qualitatively alter the results, but it is significant that the fit is better using our form than the more usual $\cos^2$ form. We believe this is evidence that in the Cr_2O_3, the spin-flop is close to being able to provide an exchange bias, but that reversal of the FM magnetization is sufficient to "reset" the bias in the opposite direction by precession of the AF spins in the Schulthess and Butler framework.[8]

Our model clearly reproduces the most striking feature of our experimental results and those of Fitzsimmons *et al.* in FeF_2 (Ref. 11)—that the exchange bias occurs orthogonal to this spin-flop direction. The most relevant analytic model is that of Nowak *et al.*[27] in which a domain state is established during field cooling which is sufficient to establish a net spin imbalance on the Cr_2O_3 surface. This spin imbalance necessarily points along the spin direction of the AF and conse-

quently this is the direction in which exchange bias is observed. We suggest that for smooth compensated interfaces the bias constant D is small and hence high energy AF spin rearrangements are required to introduce a significant net spin to the surface. Whereas, for uncompensated surfaces D will increase as the surface becomes smoother and the domain wall separation increases and the consequent energy penalty required to align the AF surface spins decreases, in agreement with the results shown in Fig. 2.

The results from all the samples show that spin-flop coupling is inevitably observed where there is an in-plane AF anisotropy but exchange bias requires an uncompensated interface with sufficiently low roughness that it is not compensated by averaging. Our model specifically excludes thermal activation of the AF as an origin of enhanced coercivity and therefore does not deal with the coercivity along the bias direction, which reaches a maximum at the blocking temperature due to energy losses in the AF as discussed by Stiles and McMichael.[29]

D. Polycrystalline results

The results from the polycrystalline Cr_2O_3 sample suggest that the exchange interaction simply averages over the available crystal orientations. This is apparent in Fig. 3, in which the enhanced coercivity associated with compensated interfaces and exchange bias associated with uncompensated interfaces are present simultaneously. Comparing the epitaxial and polycrystalline materials shown in Table I, it is clear that the polycrystalline data represent median values for the epitaxial samples.

V. CONCLUSIONS

Up to now, exchange bias has been most easily observed in polycrystalline AF systems. Our results show unambiguously that for intrinsically uncompensated single-crystal interfaces, very smooth surfaces are essential for significant exchange bias.

We have also shown that, for an optimized experimental system, which combines a highly isotropic ferromagnet with an epitaxial antiferromagnet that has strong uniaxial anisotropy, we can obtain highly reproducible and systematic angular-dependent results. Using two phenomenological parameters we can quantitatively fit hysteresis loops for all field cooling and measurement angles for a particular crystal surface. This shows that, at least in hexagonal AFs such as Cr_2O_3 and Fe_2O_3, exchange bias is a consequence of frozen AF micromagnetic disorder which results in a net uncompensated surface interaction. At temperatures at which thermal activation is unimportant (i.e., well below T_N) this interaction, is independent of, and orthogonal to, the spin-flop interaction that gives rise to enhanced coercivity. It is consistent with this conclusion that an AF spin configuration with an out-of-plane component of the AF spin is favorable for a large exchange bias.

For technological application, the value of the exchange bias needs to be significantly larger than the coercivity. Interestingly, it has not been previously demonstrated that an epitaxial AF system exhibiting such bias from uncompensated interfaces (rather than highly defective compensated ones) may be required for low coercivity. The results shown in this paper should improve the understanding of technological exchange bias systems and may assist in the development of improved materials and heterostructures.

ACKNOWLEDGMENTS

This work was supported by Samsung Electronics and the Engineering and Physical Sciences Research Council.

*Author to whom correspondence should be addressed. Electronic address: jhdho@mail.knu.ac.kr
†Electronic address: mb52@cam.ac.uk

[1] A. E. Berkowitz and K. Takano, J. Magn. Magn. Mater. **200**, 552 (1999).
[2] J. Nogués and I. K. Schuller, J. Magn. Magn. Mater. **192**, 203 (1999).
[3] V. Skumryev, S. Stoyanov, Y. Zhang, G. Hadjipanayis, D. Givord, and J. Nogues, Nature **423**, 850 (2003).
[4] W. H. Meiklejohn and C. P. Bean, Phys. Rev. **102**, 1413 (1956).
[5] A. P. Malozemoff, Phys. Rev. B **35**, R3679 (1987).
[6] D. Mauri, H. C. Siegmann, P. S. Bagus, and E. Kay, J. Appl. Phys. **62**, 3047 (1987).
[7] N. C. Koon, Phys. Rev. Lett. **78**, 4865 (1997).
[8] T. C. Schulthess and W. H. Butler, Phys. Rev. Lett. **81**, 4516 (1998).
[9] T. C. Schulthess and W. H. Butler, J. Appl. Phys. **85**, 5510 (1999).
[10] T. J. Moran, J. Nogués, D. Lederman, and I. K. Schuller, Appl. Phys. Lett. **72**, 617 (1998).
[11] M. R. Fitzsimmons, C. Leighton, J. Nogues, A. Hoffmann, K. Liu, C. F. Majkrzak, J. A. Dura, J. R. Groves, R. W. Springer, P. N. Arendt, V. Leiner, H. Lauter, and I. K. Schuller, Phys. Rev. B **65**, 134436 (2002).
[12] M. Grimsditch, A. Hoffmann, P. Vavassori, Hongtao Shi, and D. Lederman, Phys. Rev. Lett. **90**, 257201 (2003).
[13] P. Borisov, A. Hochstrat, X. Chen, W. Kleemann, and C. Binek, Phys. Rev. Lett. **94**, 117203 (2005).
[14] J. Sort, V. Langlais, S. Doppiu, B. Dieny, S. Suriñach, J. S. Muñoz, M. D. Baró, Ch. Laurent, and J. Nogués, Nanotechnology **15**, S211 (2004).
[15] R. K. Zheng, H. Liu, Y. Wang, and X. X. Zhang, J. Appl. Phys. **96**, 5370 (2004).
[16] R. Jungblut, R. Coehoorn, M. T. Johnson, Ch. Sauer, P. J. van der Zaag, A. R. Ball, Th. G. S. M. Rijks, J. ann de Stegge, and A. Reinders, J. Magn. Magn. Mater. **148**, 300 (1995).
[17] S. Dubourg, N. Negre, B. Warot, E. Snoeck, M. Goiran, J. C. Ousset, and J. F. Bobo, J. Appl. Phys. **87**, 4936 (2000).
[18] Y. Ijiri, J. A. Borchers, R. W. Erwin, S.-H. Lee, P. J. van der Zaag, and R. M. Wolf, Phys. Rev. Lett. **80**, 608 (1998).

[19] J. Nogués, T. J. Moran, D. Lederman, I. K. Schuller, and K. V. Rao, Phys. Rev. B **59**, 6984 (1999).
[20] J. Dho, C. W. Leung, Z. H. Barber, and M. G. Blamire, Phys. Rev. B **71**, 180402(R) (2005).
[21] N. J. Gokemeijer, R. L. Penn, D. R. Veblen, and C. L. Chien, Phys. Rev. B **63**, 174422 (2001).
[22] P. Steadman, M. Ali, A. T. Hindmarch, C. H. Marrows, B. J. Hickey, S. Langridge, R. M. Dalgliesh, and S. Foster, Phys. Rev. Lett. **89**, 077201 (2002).
[23] J. A. Borchers, Y. Ijiri, D. M. Lind, P. G. Ivanov, R. W. Erwin, A. Qasba, S. H. Lee, K. V. O'Donovan, and D. C. Dender, Appl. Phys. Lett. **77**, 4187 (2000).
[24] L. M. Corliss, J. M. Hastings, R. Nathans, and G. Shirane, J. Appl. Phys. **36**, 1099 (1965).
[25] M. Fiebig, D. Fröhlich, and H.-J. Thiele, Phys. Rev. B **54**, R12681 (1996).
[26] A. Hochstrat, Ch. Binek, X. Chen, and W. Kleemann, J. Magn. Magn. Mater. **272-276**, 325 (2004).
[27] U. Nowak, K. D. Usadel, J. Keller, P. Miltényi, B. Beschoten, and G. Güntherodt, Phys. Rev. B **66**, 014430 (2002).
[28] J. Camarero, J. Sort, A. Hoffmann, J. M. García-Martín, B. Dieny, R. Miranda, and J. Nogués, Phys. Rev. Lett. **95**, 057204 (2005).
[29] M. D. Stiles and R. D. McMichael, Phys. Rev. B **63**, 064405 (2001).
[30] Y. Ijiri, J. Phys.: Condens. Matter **14**, R947 (2002).